NASA TECHNICAL MEMORANDUM

NASA TM X-3226

NASA TM X-3226

COMPARISON UNDER A SIMULATED SUN OF TWO BLACK-NICKEL-COATED FLAT-PLATE SOLAR COLLECTORS WITH A NONSELECTIVE BLACK-PAINT-COATED COLLECTOR

Frederick F. Simon

Lewis Research Center
Cleveland, Ohio 44135

NATIONAL AERONAUTICS AND SPACE ADMINISTRATION • WASHINGTON, D. C. • JUNE 1975

1. Report No.	2. Government Accession No.	3. Recipient's Catalog No.
NASA TM X-3226		

4. Title and Subtitle	5. Report Date
COMPARISON UNDER A SIMULATED SUN OF TWO BLACK-NICKEL-COATED FLAT-PLATE SOLAR COLLECTORS WITH A NONSELECTIVE BLACK-PAINT-COATED COLLECTOR	June 1975
	6. Performing Organization Code
7. Author(s)	8. Performing Organization Report No.
Frederick F. Simon	E-8236
	10. Work Unit No.
9. Performing Organization Name and Address	
Lewis Research Center National Aeronautics and Space Administration Cleveland, Ohio 44135	11. Contract or Grant No.
	13. Type of Report and Period Covered
12. Sponsoring Agency Name and Address	Technical Memorandum
National Aeronautics and Space Administration Washington, D. C. 20546	14. Sponsoring Agency Code

15. Supplementary Notes

16. Abstract

A performance evaluation was made of two, black-nickel-coated, flat-plate solar collectors. Collector performance was determined under a simulated sun for a wide range of inlet temperatures, including the temperature required for solar-powered absorption air conditioning. For a basis of comparison a performance test was made on a traditional, two-glass, nonselective, black-paint-coated, flat-plate collector. Performance curves and performance parameters are presented to point out the importance of the design variables which determine an efficient collector. A black-nickel-coated collector was found to be a good performer at the conditions expected for solar-powered absorption air conditioning. This collector attained a thermal efficiency of 50 percent at an inlet temperature of 366 K (200^{o} F) and an incident flux of 946 watts/m^2 (300 Btu/hr-ft^2).

17. Key Words (Suggested by Author(s))

Solar collectors
Black-nickel coating

18. Distribution Statement

Unclassified - unlimited
STAR category 34 (rev.)

19. Security Classif. (of this report)	20. Security Classif. (of this page)	21. No. of Pages	22. Price*
Unclassified	Unclassified	23	$3.25

* For sale by the National Technical Information Service, Springfield, Virginia 22151

COMPARISON UNDER A SIMULATED SUN OF TWO BLACK-NICKEL-COATED FLAT-PLATE SOLAR COLLECTORS WITH A NONSELECTIVE BLACK-PAINT-COATED COLLECTOR

by Frederick F. Simon

Lewis Research Center

A performance evaluation was made of two, black-nickel-coated, flat-plate solar collectors. Collector performance was determined under a simulated sun for a wide range of inlet temperatures, including the temperature required for solar-powered absorption air conditioning. For a basis of comparison a performance test was made on a traditional, two-glass, nonselective, black-paint-coated, flat-plate collector. Performance curves and performance parameters are presented to point out the importance of the design variables which determine an efficient collector. A black-nickel-coated collector was found to be a good performer at the conditions expected for solar-powered absorption air conditioning. This collector attained a thermal efficiency of 50 percent at an inlet temperature of 366 K (200° F) and an incident flux of 946 watts/m^2 (300 Btu/hr-ft^2).

INTRODUCTION

An area presently being investigated by the NASA Lewis Research Center in its efforts to aid in the utilization of alternate energy sources is the use of solar energy for the heating and cooling of buildings. An important phase of the solar heating and cooling effort at Lewis is testing flat-plate collectors, which have the potential to be economical and reliable. Efficient collectors will be an important consideration in the realization of effective solar-cooling systems.

One approach for obtaining collectors which can be efficient at temperatures required in solar-cooling systems (~380 K; 225° F) is to reduce the thermal radiation loss. One manner of doing this is to use selective coatings which will be good absorbers of solar radiation and poor emitters of thermal radiation in the infrared region. A coating with high promise for achieving excellent selective properties is black nickel. Property determinations of the coating (refs. 1 and 2) and theoretical collector calculations (ref. 2) indicate that a black-nickel collector can have the properties needed for an effi-

cient solar collector. The test results of two such collectors which were tested by using the Lewis solar simulator are presented in this report.

DESCRIPTION OF COLLECTORS

The two selectively coated collectors were a two-glass, black-nickel-coated collector (2GBN) and a two-Tedlar, black-nickel-coated collector (2TBN). In order to establish a reference base, a two-glass, black-paint-coated collector (2GBP) with the same design and dimensions as the 2GBN collector was also tested. All three collectors employed aluminum tube sheets for the absorber plate. The 2GBN and the 2GBP collectors were prepared for Lewis by Honeywell, Inc., under contract, and the 2TBN collector was fabricated by the NASA Marshall Space Flight Center and supplied to Lewis for testing.

The 2GBN and 2GBP collectors had an overall dimension of 1.2 m by 1.2 m (4 ft by 4 ft), a window area of 1.39 m^2 (15 ft^2), and an absorber area of 1.25 m^2 (13.5 ft^2). The sheet-metal box of the 2GBN and 2GBP collectors had a depth of 0.165 m ($6\frac{1}{2}$ in.) with 0.076 m (3 in.) of fiberglass insulation. The aluminum absorber plate was made for Honeywell, Inc., by the Olin Brass Company and had a tube spacing of 0.0826 m ($3\frac{1}{4}$ in.). Figure 1 shows the collector on the test stand.

The 2TBN collector had an overall dimension of 1.16 m by 0.63 m by 0.12 m ($45\frac{5}{8}$ in. by $24\frac{7}{8}$ in. by $4\frac{3}{4}$ in.), a window area of 0.688 m^2 (7.4 ft^2), and an absorber plate area of 0.565 m^2 (6.08 ft^2). The aluminum box contained 0.076 m (3 in.) of Styrofoam insulation with 0.0127 m (1/2 in.) of high-temperature insulation directly in back of the absorber plate. The aluminum absorber plate had a tube spacing of 0.0254 m (1 in.). The Tedlar sheets were reinforced by a 2.5-mm- (1/10-in.-) diameter wire mesh. Figure 2 shows the disassembled 2TBN collector.

EXPERIMENTAL METHOD

Experimental Facility

The facility used to experimentally determine solar collector performance is presented in figure 3. The primary components of the facility were the energy source (solar simulator), the liquid flow loop, and the instrumentation and data acquisition equipment. A summary of information describing the facility is presented in table I.

Solar Simulator

The basic rationale for the use of a solar simulator for the testing of solar collectors is given in reference 3. This approach allows for controlled conditions that make it possible to properly compare the performance of different collector types. The simulator shown in figure 3 consisted of 143, tungsten-halogen, 300-watt lamps placed in a modular array with Fresnel lenses placed at the focal distance so as to collimate the radiation. A comparison of spectral characteristics of the simulator output with air-mass 2 sunlight is given in table II. This comparison demonstrates that the solar simulator did an excellent job of simulating the sun's radiation. More detailed information is given in references 3 to 5.

Liquid Flow Loop

The flow loop consisted of storage and expansion tanks, a pump, a heater, a test collector, and the required piping and is shown schematically in figure 4. The hot-fluid storage tank was a commercially available water heater for home use. The tank had two electrical immersion heaters, 5 kW each, and had a capacity of 0.3 m^3 (80 gal). The pump was a gear-type unit driven by a 0.19-kW (1/4-hp) electric motor through a variable-speed drive.

A heat exchanger, using city water as a coolant, was used to control the temperature of the collector coolant fluid at the collector inlet.

A mixture of ethylene glycol and water was used in the liquid loop. The specific gravity of the mixture was checked with a precision-grade hydrometer. In order to suppress vapor formation, the entire flow loop was pressurized to approximately 1.035×10^5 N/m^2 gage (15 psig) by applying a regulated inert-gas pressure to the top of the expansion tank.

The collector to be tested was mounted on a support stand that allowed rotation about either the horizontal or vertical axis. This permitted variation of the incident angle of the radiant energy to simulate both seasonal and daily variations, if desired.

Instrumentation and Data Acquisition

The parameters needed to evaluate collector performance are liquid flow rate, liquid inlet and outlet temperatures, simulated solar flux, wind speed, and ambient temperature. The flow rate was determined with a calibrated turbine-type flowmeter that had an accuracy better than 1 percent of the indicated flow. The collector inlet and out-

let temperatures were measured with ISA type-E thermocouples (Chromel-constantan). The thermocouples were calibrated at 273 and 373 K (32° and 212° F). The error in absolute temperature measurement was less than 0.5 K (1° F), and the differential temperature error between the inlet and outlet thermocouples was less than 0.1 K (0.2° F).

The ambient temperature was measured with an ISA type-E thermocouple mounted in a radiation shield. The simulated solar flux was measured with a water-cooled Gardon-type radiometer having a sapphire window. The radiometer was calibrated with a National Bureau of Standards irradiance standard.

In addition to these measurements of the basic parameters, the following parameters were also measured for the purpose of obtaining detailed information:

(1) Collector absorber plate temperatures

(2) Collector glass temperatures

(3) Collector pressure and pressure drop

(4) Temperatures of surroundings

The millivolt-level electrical outputs of the measuring instruments were recorded on magnetic tape by means of a high-speed data acquisition system. The information from the tape was sent to a digital computer for data reduction and computation. The computer results were printed out in the test facility within minutes after the data were initially recorded.

Test Procedure

The collectors were mounted on the test stand and positioned so that the radiant flux was normal to the collector. The tilt angle of the collector was 57°. The flow rate was adjusted to a value corresponding to 13.6 g/sec-m^2 (10 lb/hr-ft^2) of collector absorber area. Before the simulator was turned on, the collector was given time to achieve thermal equilibrium at the inlet temperature chosen (1 hr or more). After thermal equilibrium was established for a given inlet temperature, the simulator was turned on and the desired radiant flux was obtained by adjusting the lamp voltage. After steady-state conditions occurred, usually in 10 to 15 minutes, data were recorded. The radiant flux was then readjusted to a second value at the same collector inlet temperature, steady-state conditions were obtained, and data were again recorded. The collector inlet temperature was then reset and the procedure repeated.

Correlative Method

Justification for the method of correlating collector test data is presented in reference 3. Basically, the method involves using analytical equations that describe collector performance. The three equations useful for the determination of collector performance are as follows:

$$\eta = \alpha\tau - \frac{U_L(\overline{T}_p - T_a)}{q_i} \tag{1}$$

$$\eta = F' \left[\alpha\tau - \frac{U_L(\overline{T}_f - T_a)}{q_i}\right] \tag{2}$$

$$\eta = F_R \left[\alpha\tau - \frac{U_L(T_1 - T_a)}{q_i}\right] \tag{3}$$

These equations have the same basic form of

$$\eta = a_o - \frac{b_o(T - T_a)}{q_i} \tag{4}$$

where $(T - T_a)$ differs in the three equations by the use of $\overline{T}_p$, $\overline{T}_f$, or T_1. (All symbols are defined in appendix A.) By plotting data in the form of equation (4), (η against $(T - T_a)/q_i$), one is able to obtain valuable insight into collector performance from a knowledge of the intercept and slope of the data correlating line. In this way the values of $\alpha\tau$, U_L, F', and F_R can be obtained. As explained in reference 3, these factors will give specific information on why a collector excelled or why it performed poorly.

RESULTS AND DISCUSSION

The efficiency of each collector was calculated with the following equation:

$$\eta = \frac{GC_p(T_0 - T_1)}{q_i} \tag{5}$$

The flow rate G in equation (5) is based on the flow rate per unit of absorber area. The efficiency determined for a constant flow rate of 13.6 g/sec-m^2 (10 lb/hr-ft^2) was plotted against the ratio of temperature difference to heat flux for plate temperatures

from 307 to 376 K (94° to 218° F), average fluid temperatures from 306 to 375 K (91° to 215° F), and inlet temperatures from 301 to 371 K (83° to 208° F). Plots of these data for the three collectors tested are shown in figures 5 to 7.

The wind coefficient of 17.0 W/m^2-K (3.0 Btu/hr-ft^2-°F) shown in these plots was obtained by following the approach outlined in reference 3. This involves a determination of the outer-window convection loss from the knowledge of total heat loss, conduction loss, and radiation loss. The convection loss resulting from winds moving across a collector is one of the factors that determine collector performance; it should be stated. The present experiments maintained a constant wind speed for all the collectors. The wind coefficient given is equivalent to a wind speed of 1.6 km/hr (7mph).

The average plate temperatures used for figures 5(a), 6(a), and 7(a) were determined from an arithmetic average of 11 plate thermocouple readings in the case of the 2GBN and 2GBP collectors and five plate thermocouple readings for the 2TBN collector. The average fluid temperatures of figures 5(b), 6(b), and 7(b) were calculated by the following equation:

$$T_f = (T_0 - T_1)K + T_1 \tag{6}$$

where

$$K = \frac{GC_p}{F'U_L}\left(\frac{F'}{F_R} - 1.0\right)^1$$

The value of K was close to 1/2, which would have justified the use of an arithmetic average with little loss in accuracy.

As indicated in the discussion of equations (1) to (3), the plots shown in figures 5 to 7 differ by the values of the slope and the intercept. From a comparison of the plots, it can be seen that for a given value of efficiency, ambient temperature, and flux, the average plate temperature was slightly greater than the average fluid temperature, which in turn was greater than the inlet temperature. These differences are due to such factors as plate fin efficiency, fluid heat-transfer coefficient, and collector heat loss.

Before discussing the collector parameters determined from figures 5 to 7, it is useful to compare the three collectors in terms of an easily obtainable variable, the inlet temperature T_1. This is shown in figure 8, where it is clear that for a given inlet temperature, ambient temperature, and flux level, the best performance is provided by the 2GBN collector. Another way to demonstrate this is shown in table III, where collector performance is given for the temperature level required for solar-powered absorption air conditioning.

---

[1] See appendix B.

As previously indicated, the values of the slopes and intercepts in figures 5 to 7 give valuable insight into collector performance. From the values of the intercepts and slopes in figures 5 to 7, we are able to calculate the basic collector parameters shown in table IV. These parameters give the first clear indication of why this particular 2TBN collector did not achieve the expected performance. While table IV shows a slightly greater heat loss for the 2TBN collector than for the 2GBN collector, the main deficiency of the 2TBN collector is the low value of the product of absorptivity and transmittance. Although some of the fault for the lower-than-expected product can be attributed to the wire mesh (7 percent decrease in transmittance), the value of the absorptivity is suspected of being the greatest single reason for the low value of the product. Table IV shows that the values of F' and F_R for the 2GBN and 2GBP collectors compare well with each other. This was expected because of the common design of these two collectors. The 2TBN collector has slightly higher values of F' and F_R because the tube-to-tube distance is smaller than for the 2GBN and 2GBP collectors.

Table IV lists the values of the collector parameters F', F_R, and U_L at plate temperatures of 311 and 366 K (100° and 200° F). It is worthwhile to note that F' and F_R are weak functions of plate temperature and that U_L is a very definite function of plate temperature. This observation is further justified by the theoretical values of U_L in table IV. These theoretical values of U_L are lower than the experimental values, which is probably due to greater free convection than predicted.

A final judgement can be made on these collectors from measurement and calculation of the absorptivity of the coating. From a measurement of the amount of simulator radiation transmitted through the glazing material, values of transmittance were determined (table V). By using these values and the method of Whillier (ref. 6), absorptivity was determined from the products of $\alpha\tau$ given in table IV. The resulting calculated absorptivities are compared to the measured values of absorptivity in table V. Measured and calculated absorptivities compare very well and clearly point out why less than expected performance was achieved with the 2TBN collector.[2] The 2TBN collector had a lower than desired absorptivity.

Since the transmittance of a Tedlar sheet (0.86) is close to that of the glass used in the 2GBN and 2GBP collectors (0.89), the greatest single improvement to the 2TBN collector would be to increase the absorptivity. Other improvements in the 2TBN collector would be to decrease edge heat losses by keeping the absorber plate sides about 2.5 cm (1 in.) away from the collector box sides and by placing insulation at the sides between window and plate and to use a thinner gage Tedlar is possible and less reinforcing wire.

By using in equation (3) the values of absorptivity and heat loss of the 2GBN col-

---

[2]The agreement between calculated and measured absorptivities for spectrally sensitive surfaces is further evidence of the simulator's ability to give a good spectral simulation of the sun.

lector, a potential performance curve for the 2TBN collector can be obtained, as shown in figure 9. Versions of the 2TBN collector which incorporate the improvements given in the preceding paragraph should allow a level of performance shown by the dashed line in figure 9. The merit of these suggested improvements is best shown by comparing the results of the present 2GBN collector with the initial version of this collector in figure 9. The initial 2GBN collector gave lower performance than had been expected because of heat losses caused by the absorber plate being close to metal supports and the edge of the collector box and by a lower-than-desired absorptivity (0.88). An improved box design and a larger value of absorptivity resulted in the present much-improved performance curve.

An important design variable is the no-flow collector plate temperature. This can be determined by applying the zero efficiency condition to the correlating equations plotted in figures 5 to 7. Table VI shows the no-flow plate temperatures obtained by this approach. As expected, the more efficient 2GBN collector has the highest no-flow plate temperature.

CONCLUDING REMARKS

For a collector to be a good performer at high temperatures, it is not sufficient to simply decrease collector heat loss. Factors related to the energy transmitted, absorbed, and collected must also be considered. This study presented evidence to show that a two-glass, black-nickel-coated collector did well in all aspects of collector design needed for good performance.

For the three collectors tested, the following thermal efficiencies were achieved at a fluid inlet temperature of 366 K (200° F) and a simulated incident solar flux of 946 W/m^2 (300 Btu-hr-ft^2):

(1) Two-glass, black-nickel-coated collector, 50

(2) Two-glass, black-paint-coated collector, 42

(3) Two-Tedlar, black-nickel-coated collector, 29

Lewis Research Center,
National Aeronautics and Space Administration,
Cleveland, Ohio, March 4, 1975,
506-23.

APPENDIX A

SYMBOLS

C_p heat capacity, J/g-K (Btu/lb-^oF)

F_R collector plate heat-removal efficiency, dimensionless

F' collector plate efficiency factor, dimensionless

G flow rate per unit absorber area, g/sec-m^2 (lb/hr-ft^2)

h_o wind coefficient, W/m^2-K (Btu/hr-ft^2-^oF)

L collector length, m (ft)

q_A absorbed energy, W/m^2 (Btu/hr-ft^2)

q_i incident direct solar radiation, W/m^2 (Btu/hr-ft^2)

q_u useful energy collected, W/m^2 (Btu/hr-ft^2)

T_a ambient temperature, K (^oF)

T_0 fluid outlet temperature, K (^oF)

T_1 fluid inlet temperature, K (^oF)

$\overline{T}_f$ average collector fluid temperature, K (^oF)

$\overline{T}_p$ average collector plate temperature, K (^oF)

U_L overall collector heat-loss coefficient, W/m^2-K (Btu/hr-ft^2-^oF)

α collector surface absorptivity, dimensionless

ϵ_p emissivity of collector surface

η collector efficiency, dimensionless

τ transmittance

Subscripts:

e effective

– average

APPENDIX B

DERIVATION OF AVERAGE TEMPERATURE OF COLLECTOR FLUID

From a heat balance on a differential element of a flow channel (fig. 10), the following equation was obtained:

$$q_u(x)\,dx\,\Delta y = C_p G L\,\Delta y\,dT_f \tag{B1}$$

The useful energy may be expressed as follows:

$$q_u(x) = F'\left[q_A - U_L(T_f - T_a)\right] \tag{B2}$$

By combining equations (B1) and (B2) we obtain

$$\int_{T_1}^{T_f} \frac{dT_f}{q_A - U_L(T_f - T_a)} = \int_0^L \frac{F'}{GC_pL}\,dx \tag{B3}$$

Carrying out the integration gives

$$\frac{q_u(x)}{q_u(0)} = e^{-\frac{F'U_L}{GC_p}\frac{x}{L}} \tag{B4}$$

or

$$\frac{q_A - U_L(T_f - T_a)}{q_A - U_L(T_1 - T_a)} = e^{-\frac{F'U_L}{GC_p}\frac{x}{L}} \tag{B5}$$

From equation (3) in the main text

$$\bar{q}_u = F_R\left[q_A - U_L(T_1 - T_a)\right] \tag{B6}$$

Combining equations (B5) and (B6) gives

$$T_f = \frac{\bar{q}_u}{F_R U_L} \left(1 - e^{- \frac{F' U_L}{G C_p} \frac{x}{L}} \right) + T_1 \tag{B7}$$

Defining the average fluid temperatures as

$$\bar{T}_f = \frac{1}{L} \int T \, dx \tag{B8}$$

we get, by using equation (B7),

$$\bar{T}_f = \left(\frac{\bar{q}_u}{F_R U_L} \right) \frac{1}{L} \int_0^L \left(1 - e^{- \frac{F' U_L}{G C_p} \frac{x}{L}} \right) dx + T_1 \tag{B9}$$

which results in

$$\bar{T}_f = \frac{\bar{q}_u}{F_R U_L} \left[1 + \frac{G C_p}{F' U_L} \left(e^{- \frac{F' U_L}{G C_p}} - 1 \right) \right] + T_1 \tag{B10}$$

Substituting

$$\bar{q}_u = G C_p (T_0 - T_1) \tag{B11}$$

into (B10), we obtain, after rearranging,

$$\bar{T}_f = (T_0 - T_1) K + T_1 \tag{B12}$$

where

$$K = \frac{G C_p}{F' U_L} \left(\frac{F'}{F_R} - 1 \right) \tag{B13}$$

REFERENCES

1. McDonald, G. E.: Spectral Reflectance Properties of Black Chrome for Use as a Solar Selective Coating. Presented at U.S. Section Annual Meeting of the International Solar Energy Society, Fort Collins, Colo., Aug. 19-23, 1974.

2. Contract NAS3-17862, Development of Flat Plate Solar Collectors for the Heating and Cooling of Buildings. Progress Rept. 3 and 4, Honeywell, Inc., Nov.-Dec. 1973.

3. Simon, F. F.; and Harlemert, P.: Flat-Plate Collector Performance Evaluation. The Case for a Solar Simulation Approach. Presented at U.S. Section Annual Meeting of the International Solar Energy Society, Cleveland, Oh., Oct. 3-4, 1973.

4. Yass, K.; and Curtis, H. B.: Low-Cost, Air Mass 2 Solar Simulator. NASA TM X-3059, 1974.

5. Vernon, R. W.; and Simon, F. F.: Flat-Plate Collector Performance Determined Experimentally with a Solar Simulator. Presented at U.S. Section Annual Meeting of the International Solar Energy Society, Fort Collins, Colo., Aug. 19-23, 1974.

6. Whillier, A.: Design Factors Influencing Solar Collector Performance. American Society of Heating, Refrigeration, and Air Conditioning Engineering, Technical Committee on Solar Energy Utilization, 1967, pp. 27-40.

TABLE I. - DESCRIPTION OF LEWIS SOLAR SIMULATOR

Radiation source:	
Number of lamps	143
Power (each lamp), W	300
Coating	Tungsten-halogen
Total divergence angle, deg	9
Test area, m	10 by 10
Test condition limits:	
Flux, W/m^2 ($Btu/hr-ft^2$)	473 - 1103 (150 - 350)
Flow, m^3/min (gal/min)	3.79×10^{-3} (1)
Inlet temperature, K (^oF)	297 - 372 (75 - 210)
Wind velocity, km/hr (mph)	0 - 2.3 (0 - 10)

TABLE II. - COMPARISON OF SOLAR SIMULATOR AND AIR-MASS 2 SUNLIGHT

	Air-mass 2 sunlight	Solar simulator
Energy output, percent:		
Ultraviolet	2.7	0.3
Visible	44.4	48.4
Infrared	52.9	51.3
Energy uses:		
Absorptivity (selective surface)	0.90	0.90
Glass transmission	.85	.86
Reflectivity of aluminum mirror	.86	.88
Solar-cell efficiency, percent	12.6	13.4

TABLE III. - COMPARISON OF COLLECTOR EFFICIENCIES

[Flux, 946 W/m^2 (300 $Btu/hr-ft^2$).]

Collector	Inlet temperature, T_1, K (^oF)		
	302 (85)	333 (140)	366 (200)
	Efficiency, η		
Two glass, black-nickel coated	71	63	50
Two glass, black-paint coated	73	60	42
Two Tedlar, black-nickel coated	53	43	29

TABLE IV. - COLLECTOR PERFORMANCE PARAMETERS

Collector	Average collector plate temperature, $\overline{T}_p$, K (^oF)								Product of collector surface absorptivity and effective transmittance, $\alpha\tau_e$
	311 (100)	366 (200)	311 (100)	366 (200)	311 (100)		366 (200)		
	Collector plate efficiency factor, F'		Collector plate heat-removal efficiency, F_R		Overall collector heat-loss coefficient, U_L, W/m^2-K (Btu/hr-ft^2-^oF)				
					Experiment	Theory	Experiment	Theory	
Two glass, black-nickel coated	0.96	0.97	0.94	0.94	3.00 (0.53)	2.10 (0.37)	3.38 (0.60)	3.12 (0.55)	0.75
Two glass, black-paint coated	.97	.97	.93	.95	4.20 (0.74)	3.63 (0.64)	4.92 (0.87)	4.71 (0.83)	.78
Two Tedlar, black-nickel coated	1.00	.99	.95	.95	3.74 (0.66)	----- -----	4.08 (0.72)	----- -----	.56

TABLE V. - COLLECTOR RADIATION PROPERTIES

Collector	Surface absorptivity, α		Surface emissivity, ϵ	Transmittance, τ
	Measured[a]	Calculated[b]		
Two glass, black-nickel coated	0.95	0.92	0.08	0.78
Two glass, black-paint coated	.95	.93	~.95	.78
Two Tedlar, black-nickel coated	.73	.79	----	.68

[a]Measured with a spectrophotometer.

[b]Calculated from experimental value of $\alpha\tau_e$.

TABLE VI. - CALCULATED NO-FLOW

ABSORBER PLATE TEMPERATURES

[Incident direct solar radiation, q_i, 946 W/m^2 (300 Btu/hr-ft^2); ambient temperature, T_a, 302 K (85° F).]

Collector	No-flow temperature	
	K	$^\circ$F
Two glass, black-nickel coated	480	405
Two glass, black-paint coated	436	325
Two Tedlar, black-nickel coated	430	315

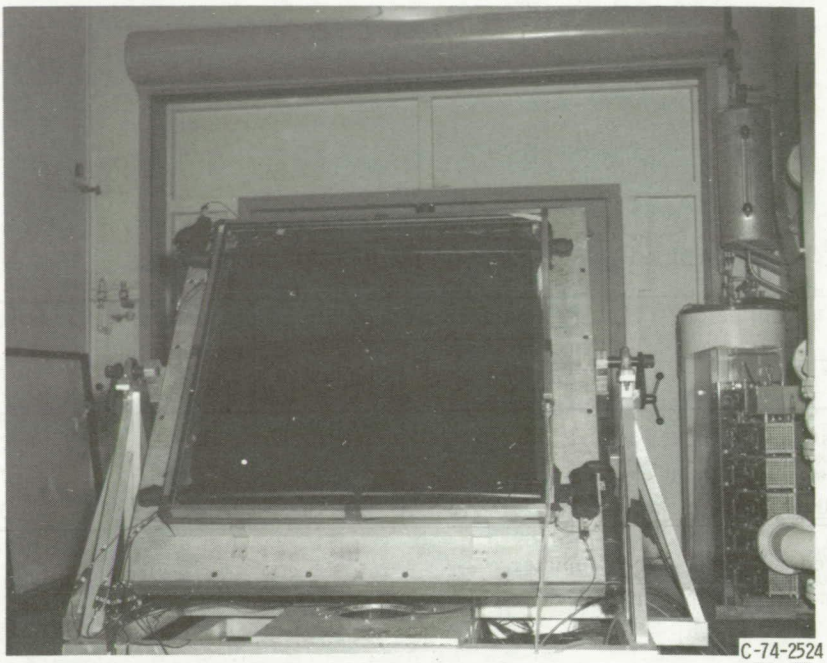

Figure 1. - Two-glass, black-nickel-coated collector.

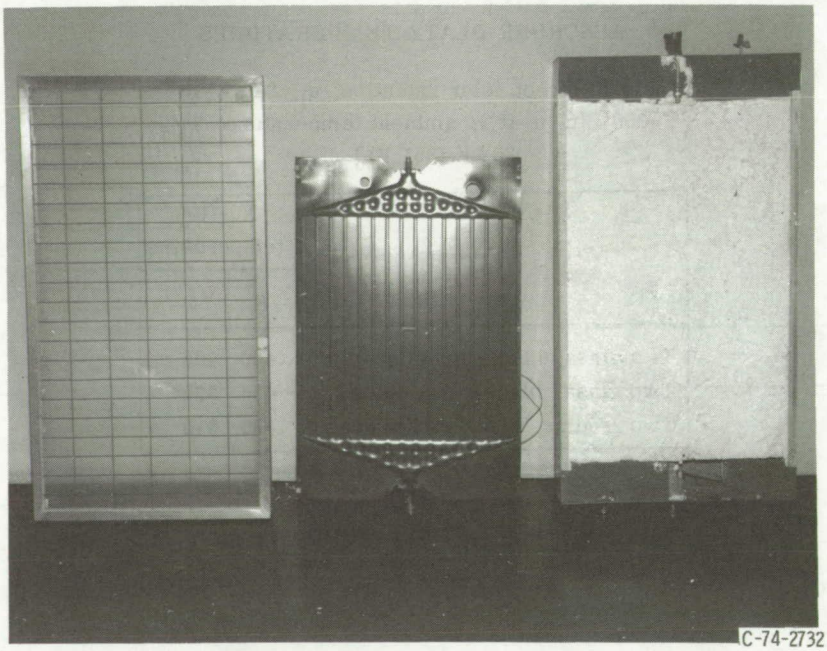

Figure 2. - Two-Tedlar, black-nickel-coated collector.

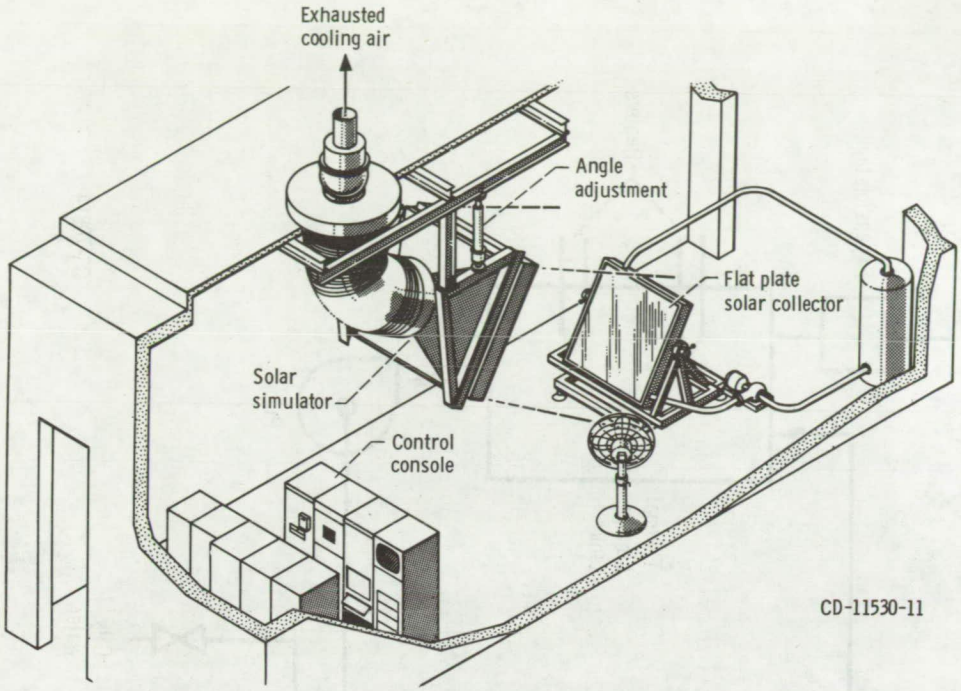

Figure 3. - Indoor facility used to experimentally determine solar collector performance.

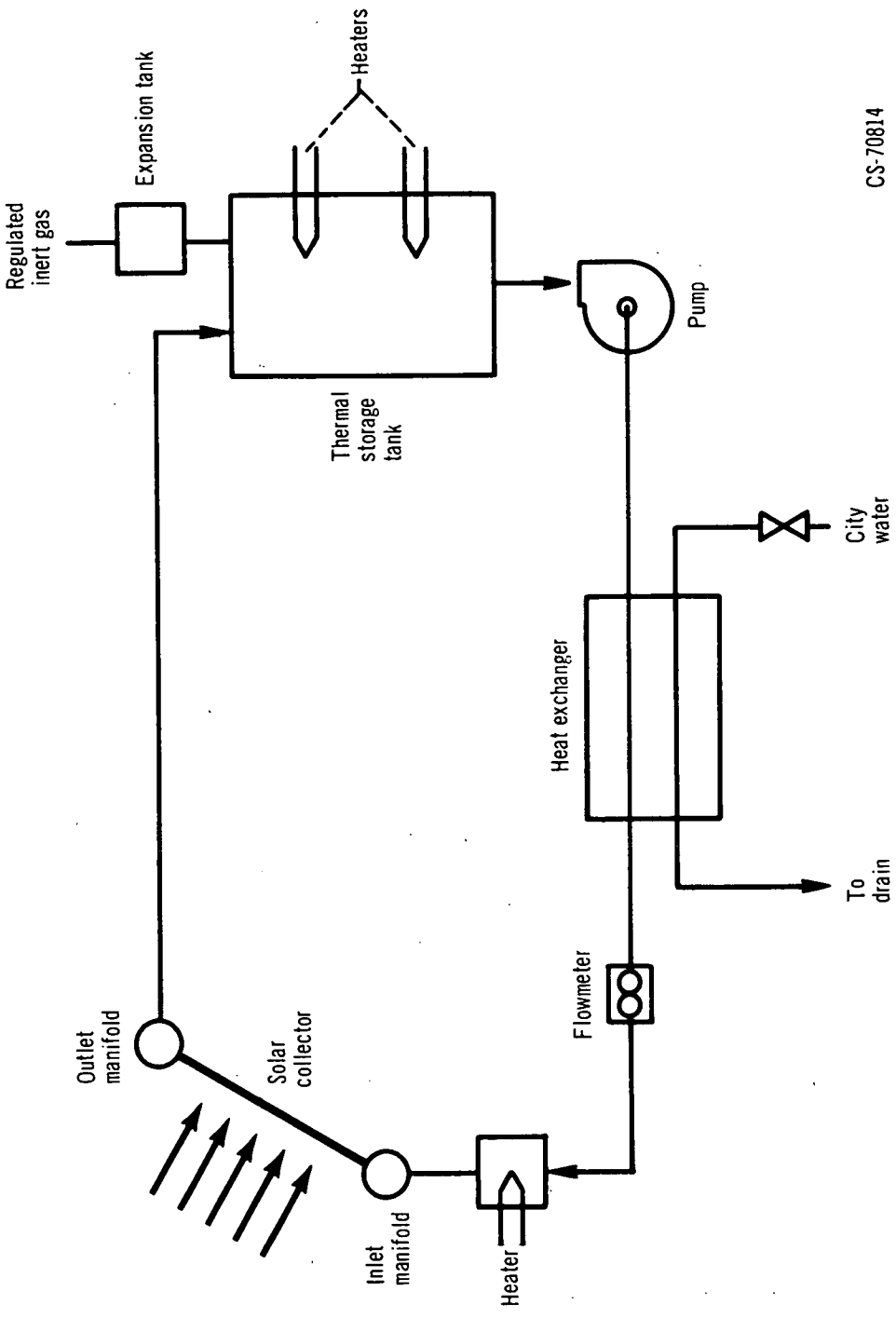

Figure 4. - Schematic of liquid flow loop.

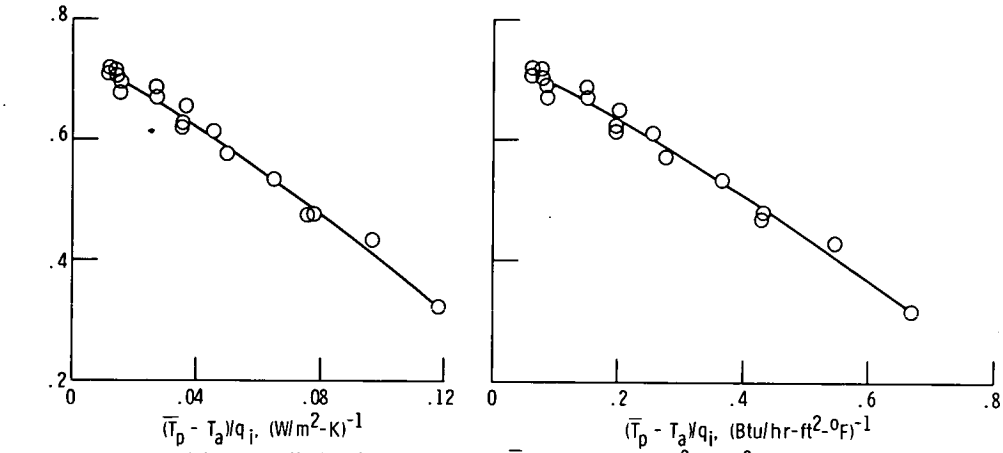

(a) Average collector plate temperature, $\overline{T}_p$, 313 to 375 K (104° to 216° F), respectively.

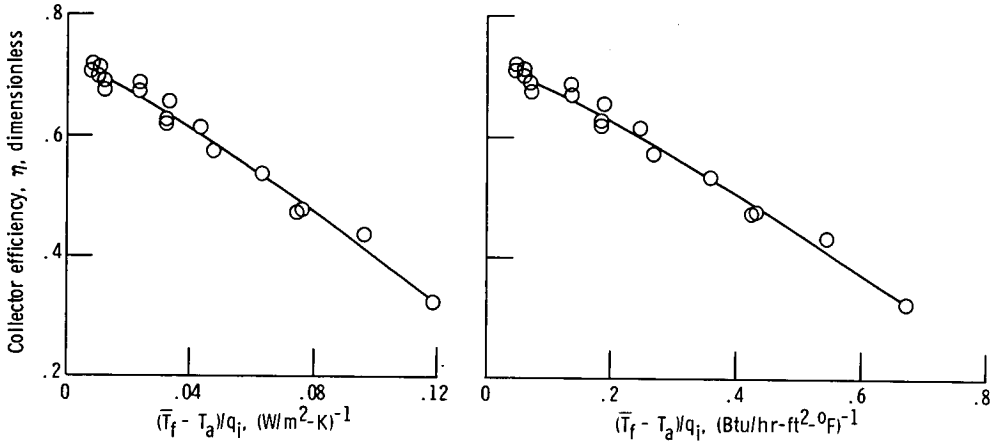

(b) Average collector fluid temperature, $\overline{T}_f$, 311 to 374 K (100° to 214° F), respectively.

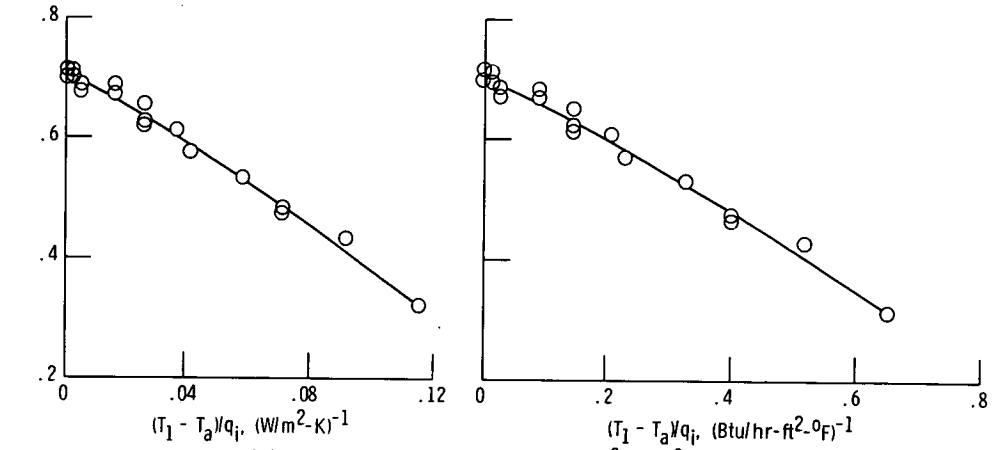

(c) Fluid inlet temperature, T_1, 305 to 370 K (90° to 206° F), respectively.

Figure 5. - Performance of two-glass, black-nickel-coated collector. Flow rate, G, 13.6 g/sec-m^2 (10 lb/hr-ft^2); ambient temperature, T_a, 302 K (85° F); incident direct solar radiation, q_i, 589 to 977 W/m^2 (187 to 310 Btu/hr-ft^2); wind coefficient, h_o, 17.0 W/m^2-K (3.0 Btu/hr-ft^{2}-°F) - where the SI (or primary) units apply to the graphs on the left and the U.S. customary (or auxiliary) units apply to the graphs on the right.

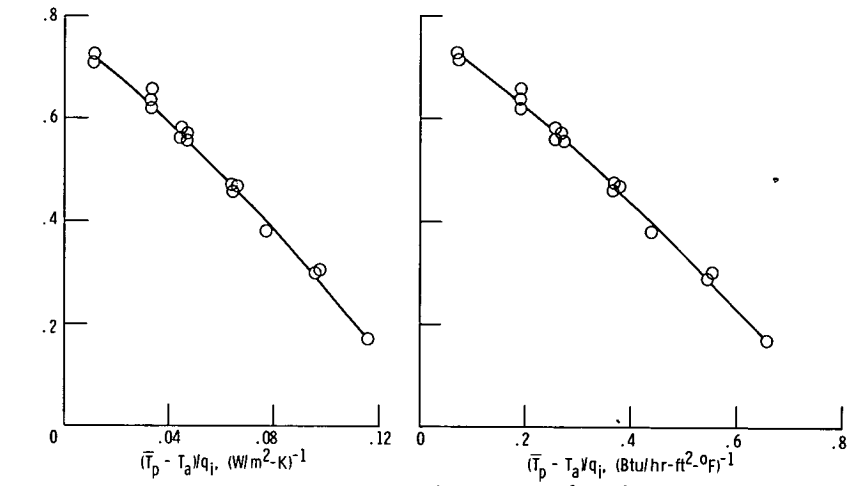

(a) Average collector plate temperature, $\bar{T}_p$, 309 to 376 K (96^o to 218^o F), respectively.

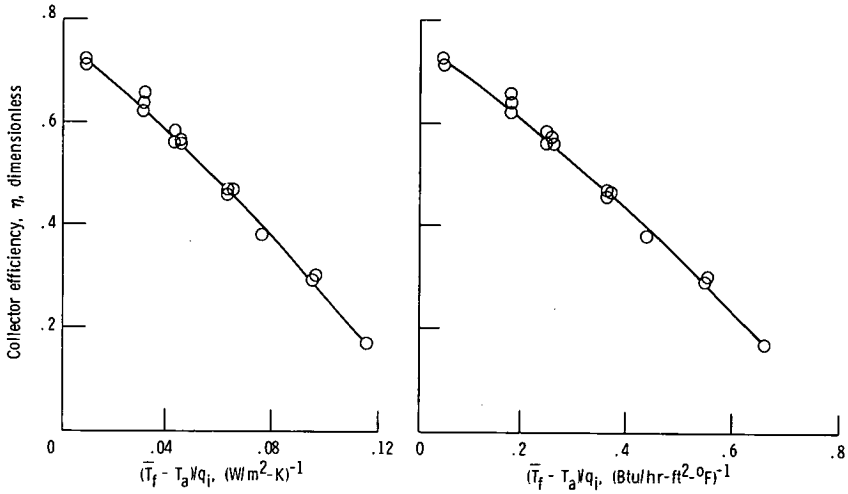

(b) Average collector fluid temperature, $\bar{T}_f$, 306 to 375 K (91^o to 215^o F), respectively.

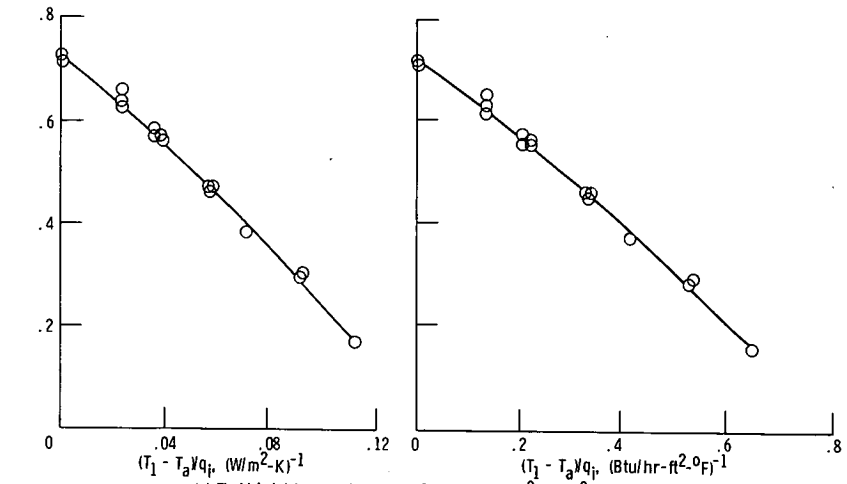

(c) Fluid inlet temperature, T_1, 301 to 371 K (83^o to 208^o F), respectively.

Figure 6. - Performance of two-glass, black-paint-coated collector. Flow rate, G, 13.6 g/sec-m^2 (10 lb/hr-ft^2); ambient temperature, T_a, 301 K (83^o F); incident direct solar radiation, q_i, 629 to 987 W/m^2 (197 to 313 Btu/hr-ft^2); wind coefficient, h_o, 17.0 W/m^2-K (3.0 Btu/hr-ft^2-^{o}F) - where the SI (or primary) units apply to the graphs on the left and the U. S. customary (or auxiliary) units apply to the graphs on the right.

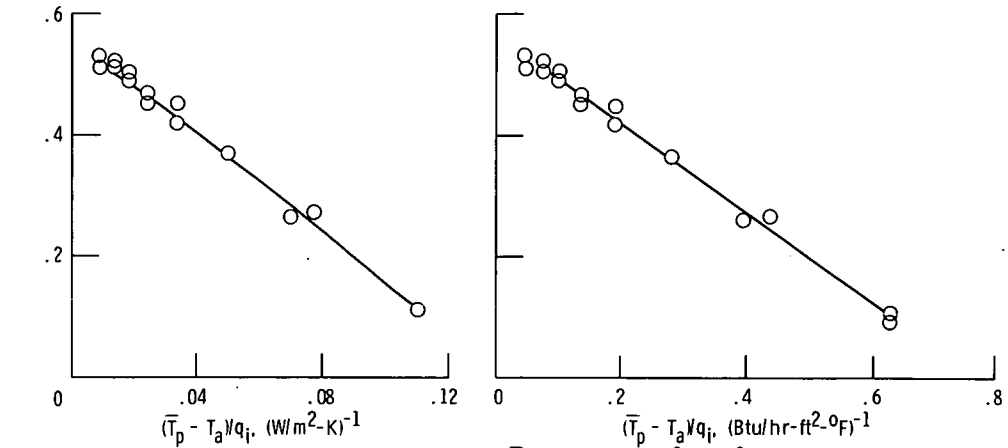

(a) Average collector plate temperature, $\bar{T}_p$, 307 to 372 K (94° to 211° F), respectively.

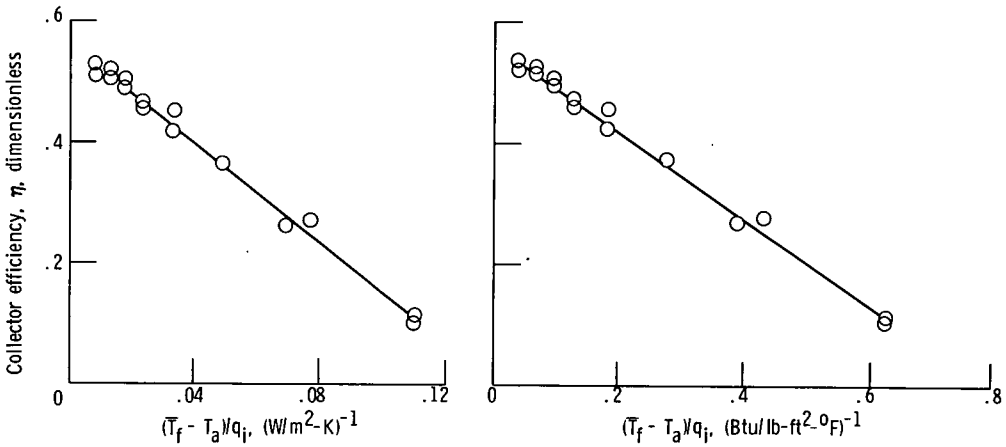

(b) Average collector fluid temperature, $\bar{T}_p$, 307 to 372 K (94° to 210° F), respectively.

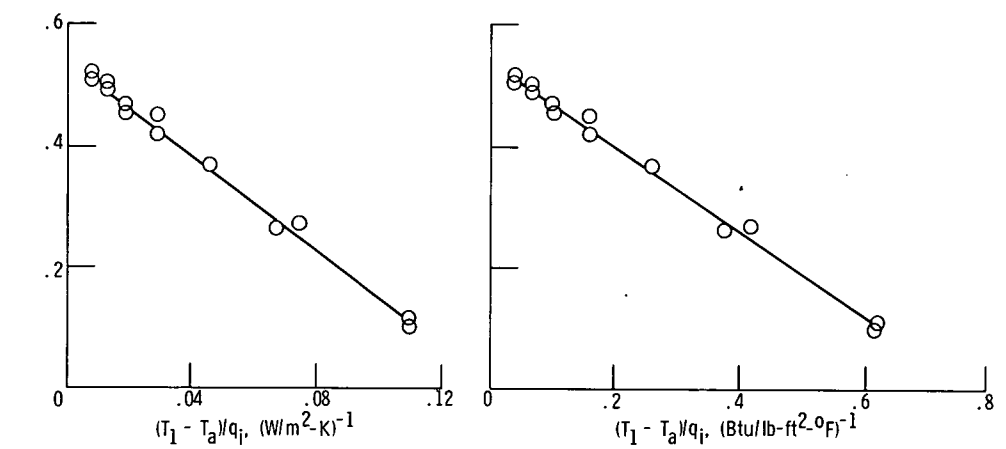

(c) Fluid inlet temperature, T_1, 304 to 369 K (88° to 205° F), respectively.

Figure 7. - Performance of two-Tedlar, black-nickel-coated collector. Flow rate, G, 13.6 g/sec-m^2 (10 lb/hr-ft^2); ambient temperature, T_a, 302 K (85° F); incident direct solar radiation, q_i, 621 to 1012 W/m^2 (197 to 321 Btu/hr-ft^2); wind coefficient, h_o, 17.0 W/m^2-K (3.0 Btu/hr-ft^2-°F) - where the SI (or primary) units apply to the graphs on the left and the U. S. customary (or auxiliary) units apply to the graphs on the right.

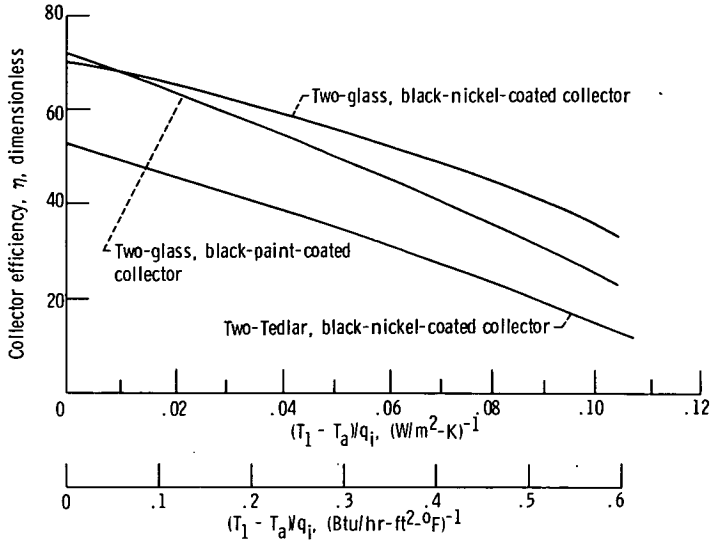

Figure 8. - Comparison of collector performance for two-glass, black-nickel-coated; two-glass, black-paint-coated; and two-Tedlar, black-nickel-coated collectors.

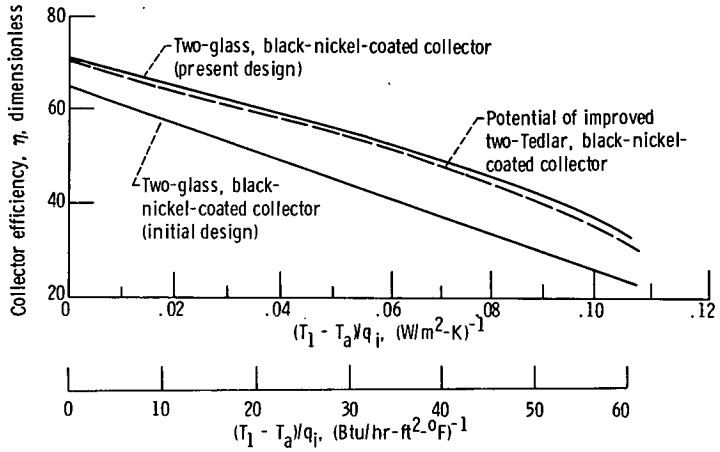

Figure 9. - Comparison of collector performance for two-Tedlar, black-nickel-coated collector and the initial and present designs of two-glass, black-nickel-coated collector.

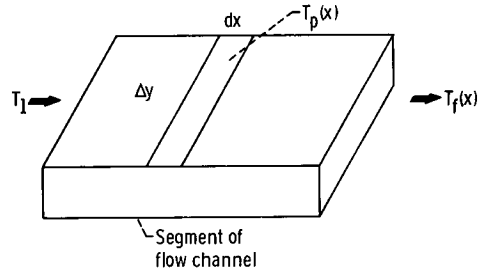

Figure 10. - Heat balance on differential element of flow channel.

NATIONAL AERONAUTICS AND SPACE ADMINISTRATION
WASHINGTON, D.C. 20546

OFFICIAL BUSINESS
PENALTY FOR PRIVATE USE $300

SPECIAL FOURTH-CLASS RATE
BOOK

POSTAGE AND FEES PAID
NATIONAL AERONAUTICS AND
SPACE ADMINISTRATION
451

U.S.MAIL

POSTMASTER: If Undeliverable (Section 158 Postal Manual) Do Not Return

"The aeronautical and space activities of the United States shall be conducted so as to contribute . . . to the expansion of human knowledge of phenomena in the atmosphere and space. The Administration shall provide for the widest practicable and appropriate dissemination of information concerning its activities and the results thereof."

—NATIONAL AERONAUTICS AND SPACE ACT OF 1958

NASA SCIENTIFIC AND TECHNICAL PUBLICATIONS

TECHNICAL REPORTS: Scientific and technical information considered important, complete, and a lasting contribution to existing knowledge.

TECHNICAL NOTES: Information less broad in scope but nevertheless of importance as a contribution to existing knowledge.

TECHNICAL MEMORANDUMS: Information receiving limited distribution because of preliminary data, security classification, or other reasons. Also includes conference proceedings with either limited or unlimited distribution.

CONTRACTOR REPORTS: Scientific and technical information generated under a NASA contract or grant and considered an important contribution to existing knowledge.

TECHNICAL TRANSLATIONS: Information published in a foreign language considered to merit NASA distribution in English.

SPECIAL PUBLICATIONS: Information derived from or of value to NASA activities. Publications include final reports of major projects, monographs, data compilations, handbooks, sourcebooks, and special bibliographies.

TECHNOLOGY UTILIZATION PUBLICATIONS: Information on technology used by NASA that may be of particular interest in commercial and other non-aerospace applications. Publications include Tech Briefs, Technology Utilization Reports and Technology Surveys.

Details on the availability of these publications may be obtained from:

SCIENTIFIC AND TECHNICAL INFORMATION OFFICE

NATIONAL AERONAUTICS AND SPACE ADMINISTRATION

Washington, D.C. 20546